Single Longitudinal Mode and Widely Tunable $Er:Y_2O_3$ Ceramic Laser at $\sim 2.7\ \mu m$

Manman Ding, Xuanxi Li, Fei Wang, Jun Wang, Deyuan Shen, Dingyuan Tang, and Heyuan Zhu

***Abstract*—We report on single-longitudinal-mode and tunable operation of an $Er:Y_2O_3$ ceramic laser at $\sim$2.7 μm using intracavity Fabry-Perot etalons combined with a birefringent filter. The laser is pumped with a high brightness, narrow linewidth diode source at $\sim$980 nm and generated over 240 mW of linearly polarized output power at 2717 nm for an absorbed pump power of 5.1 W. The wavelength tuning range demonstrated was spanned from 2708.6 nm–2741.2 nm, with output powers of $>$220 mW in the whole tuning range.**

***Index Terms*—2.7 μm, Er:Y2O3 ceramic, single-longitudinal-mode, tunability.**

I. Introduction

HIGHLY coherent mid-infrared laser sources are critical for a variety of applications in remote sensing and spectroscopy analysis. Laser wavelength around 3 μm exhibits strong absorption in many molecules of interest such as greenhouse gases and hydrocarbons, which make it attractive for environmental and biomedical gas analysis/detection [1]. Tunable narrow-linewidth lasers in this spectral regime are ideal sources to realize fast and precise measurement [1]. Therefore, development of tunable single frequency laser sources in this spectral region are of great interest and highly desirable.

Rare-earth Er^{3+} ions doped solid-state lasers are usually used to obtain these wavelengths generation ($^4I_{11/2} \rightarrow {}^4I_{13/2}$ transition) with direct pumping into the upper laser level utilizing the well-developed $\sim$980 nm laser diodes [2], [3], [4], [5], [6], [7]. Among the developed Er-doped host materials, cubic sesquioxide (Y_2O_3, Sc_2O_3 and Lu_2O_3) ceramics are attractive owing to their high thermal conductivity (e.g., 13.4 W $m^{-1}K^{-1}$ for Y_2O_3), the reduced non-radiative decay rate resulting from their low phonon energies (591 cm^{-1} for Y_2O_3), as well as the relatively lower optimum Er^{3+} doping level and hence reduced instabilities originated from heat deposition [8], [9], [10]. Compared with sesquioxides single crystals, ceramics can be prepared at temperatures much lower than the melting points, and with advantages such as volume scalability with low cost, versatile structures, and/or varying doping profiles-all of which make it suitable as widespread materials for efficient and high power $\sim$3 μm laser operation [11]. In recent years, with the development of fabrication technology, efficient $\sim$3 μm laser operation based on $Er:Y_2O_3$ and $Er:Lu_2O_3$ ceramics have been successfully demonstrated at either room temperature or with cryogenic cooling [12], [13], [14], [15], [16], [17], [18].

There are multiple technologies to obtain single longitudinal mode (SLM) lasers such as short cavity method, intracavity etalon method, twisted mode technique, nonplanar ring oscillator (NPRO), unidirectional ring lasers, and volume Bragg grating method etc. [19], [20], [21], [22], [23], [24]. Etalons-based longitudinal mode selection is a commonly used approach with advantages of simple structure, high compactness, and with flexibility to add modulation elements into the resonator to adjust output characteristics, e.g., incorporating a birefringent filter (BRF) for wider wavelength tuning. Employing a short cavity configuration, single-frequency laser operation from a 1 mm long Er:YAG crystal was demonstrated with output power of 70 mW, and by changing the Er:YAG temperature and pump power, wavelength tunability over a 1.9 nm range around 2.83 μm was realized [3]. In 2015, an Er:GGG microchip laser was demonstrated with an output power of 50.8 mW and pulsed energy of 0.306 mJ at 2.704 μm [19]. Recently, also with a microchip configuration, dual wavelength laser operation at 2717 nm and 2740 nm was realized from a 15 at.% $Er:Y_2O_3$ ceramic, generating 234.8 mW and 102 mW of output power, respectively [25]. Benefit from the reduced geometric resonator length, microchip lasers are compact with low optical loss, however, short crystal/resonator length greatly limit the pump absorption and controllability of laser. Single longitudinal mode laser operation with wide wavelength tunability in this spectral regime, which is particularly attractive for many applications, has not been demonstrated yet.

Manuscript received 11 October 2022; revised 21 December 2022; accepted 27 December 2022. Date of publication 30 December 2022; date of current version 6 January 2023. This work was supported by the National Natural Science Foundation of China NSFC under Grants 62035007, 61875078, and 62105130. *(Corresponding author: Deyuan Shen.)*

Manman Ding is with the Department of Optical Science and Engineering, Fudan University, Shanghai 200433, China, and also with the Jiangsu Collaborative Innovation Center of Advanced Laser Technology and Emerging Industry, Xuzhou 221116, China (e-mail: mm_ding@yeah.net).

Xuanxi Li, Jun Wang, and Dingyuan Tang are with the Jiangsu Key Laboratory of Advanced Laser Materials and Devices, School of Physics and Electronic Engineering, Jiangsu Normal University, Xuzhou 221116, China (e-mail: lixuanxi113@163.com; jwang025@e.ntu.edu.sg; edytang@ntu.edu.sg).

Fei Wang is with the Jiangsu Collaborative Innovation Center of Advanced Laser Technology and Emerging Industry, Xuzhou 221116, China, and also with the Jiangsu Institute of Mid Infrared Laser Technology & Applications, Xuzhou 221000, China (e-mail: hiruoyi@126.com).

Deyuan Shen is with the Jiangsu Collaborative Innovation Center of Advanced Laser Technology, Jiangsu, China, and also with the Jiangsu Key Laboratory of Advanced Laser Materials and Devices, School of Physics and Electronic Engineering, Jiangsu Normal University, Xuzhou 221116, China (e-mail: mrde@jsnu.edu.cn).

Heyuan Zhu is with the Department of Optical Science and Engineering, Fudan University, Shanghai 200433, China (e-mail: hyzhu@fudan.edu.cn).

Digital Object Identifier 10.1109/JPHOT.2022.3233189

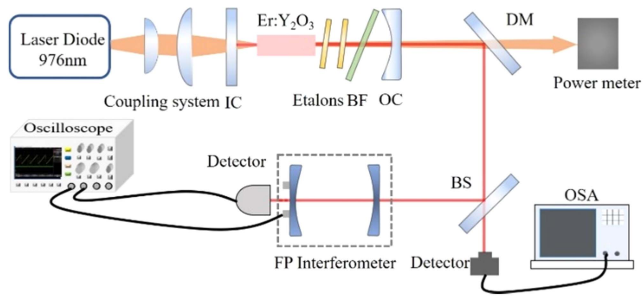

Fig. 1. Schematic diagram of Er:Y_2O_3 ceramic laser.

In this paper, we report a single frequency and tunable operation of an Er:Y_2O_3 ceramic laser with double Fabry-Perot etalons and a birefringent filter. The Er:Y_2O_3 ceramic is home developed with 3.0 at.% doping level. Pumped directly into the upper laser level ($^4I_{11/2}$) using a spectrally narrowed 976 nm laser diode, the laser generated 240 mW of SLM output power at 2717 nm for an absorbed pump power of 5.1 W. The wavelength was tuned from 2708.6 nm-2741.2 nm, and the output power was >220 mW over the whole tuning range. This work, to the best of our knowledge, represents the first SLM and widely tunable solid-state laser oscillator in the ∼3 μm spectral regime.

II. Experimental Setup

Schematic diagram of the Er:Y_2O_3 ceramic laser is shown in Fig. 1. The pump source is a high brightness 976 nm laser diode with a delivery fiber of 105 μm core and 0.22 NA. Output of the laser diode was spectrally narrowed and wavelength was stabilized with a volume Bragg grating to have a linewidth of ∼0.3 nm. Pump radiation was focused into the ceramic by a couple of spherical lenses with a focal length of 25.4 mm and 100 mm, respectively. The diameter of the pump beam inside the ceramic was ∼400 μm. The Er:Y_2O_3 ceramic was grown in house via coprecipitation process, as described in our previous work [26]. Considering the severe thermal effects in the ceramic (quantum defect of about 65%), the Er^{3+} doping level is 3.0 at.% and water-cooled by a copper heat sink maintained at ∼15 °C. The sample was cut to have a dimension of 2 × 3 × 5.5 mm^3 (5.5 mm in length), and both end faces were optically polished without antireflection coatings. Approximately 42% of the 976 nm incident pump power was absorbed after single pass the ceramic.

The Er:Y_2O_3 ceramic laser has a linear resonator structure. A plane mirror coated with a transmission of T >85% at ∼980 nm and high reflectivity of R >99.8% at the lasing wavelength (2.65 μm–2.95 μm) was used as input coupler (IC). The output coupler (OC) has 300 mm radius of curvature concave with transmission of T >85% at ∼980 nm and T = 5% transmission at the lasing wavelength. Behind the OC, a 45° dichroic mirror (DM) was used to filter the residual pump light in the output beam. Two uncoated 0.5 mm thick YAG plates were employed as longitudinal mode selector and were placed as close as possible to the ceramic where the oscillation mode beam size is larger for minimizing insertion loss. A 2 mm thick quartz birefringent filter (BF) was placed at Brewster angle into the resonator for wavelength tunability. The physical length of the resonator was ∼57 mm, resulting a mode spacing of ∼2.4 GHz. Output power and spectrum were recorded using a power meter (Ophir, 3A-PF-12) and an optical spectrum analyzer of 50 pm resolution (AQ6375B, Yokogawa).

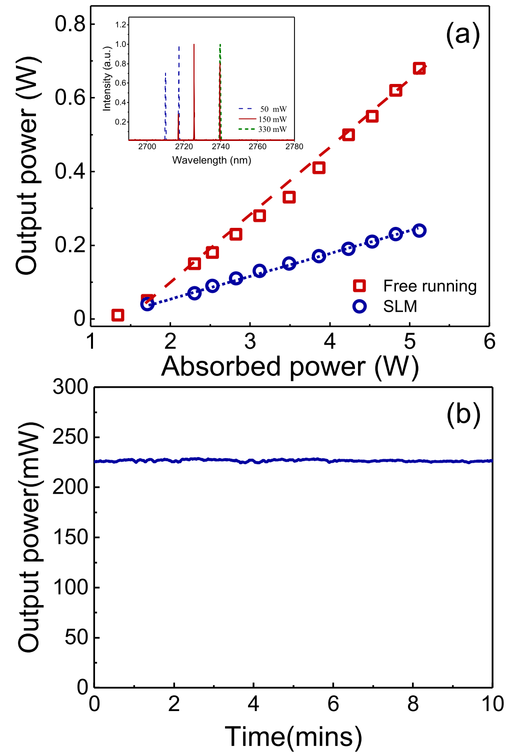

Fig. 2. (a) Output characteristics of Er:Y_2O_3 ceramic laser in free running mode and in single longitudinal mode operations and (b) power stability in 10 minutes. Inset in (a): output spectrum at different output power levels in free-running mode.

III. Experimental Results and Discussions

The Er:Y_2O_3 ceramic was first evaluated in free running mode in the absence of etalons and BF. In a short resonator scheme (physical length of ∼8 mm), oscillation threshold occurs at an absorbed power of 1.34 W. The Dependence of the output power on absorbed pump power is depicted in Fig. 2(a) (squares). The laser generated 0.68 W of output power at an absorbed power of 5.1 W, giving a slope efficiency of 18.6% with respect to the absorbed pump power. According to previous reports, this lasing efficiency is comparable with that of 7 at.% or 15 at.% doped Er:Y_2O_3 ceramics at room temperature [12], [17]. To tolerate the insertion of etalons and BF, the resonator length was then elongated to ∼57 mm with other experimental conditions unaltered. In this case, lasing threshold was nearly the same as short resonator while the slope efficiency was decreased to ∼13.7% with respect to the absorbed pump power. The larger diffraction loss and absorption loss of water vapor in air should be responsible for this degeneration. At an absorbed pump power of 5.1 W, the output power was 0.5 W.

Lasing spectrum of the ceramic laser in free-running mode was operated in multi-wavelength mode, as shown in the inset

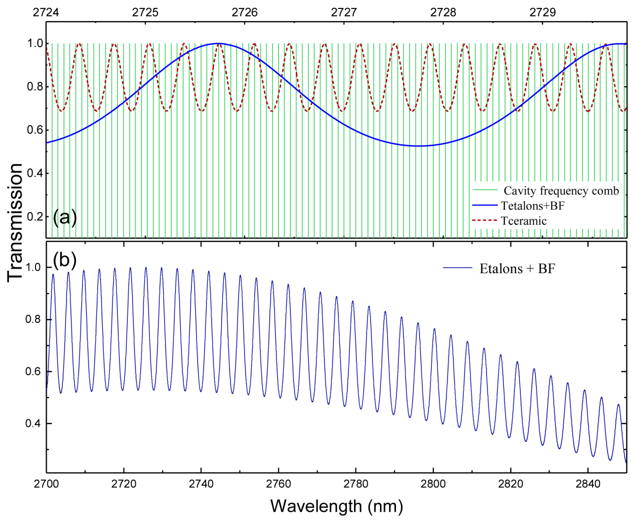

Fig. 3. (a) Comparison between the cavity frequency comb, the combined etalons and BF and the F-P effects of the uncoated ceramic. (b) Simulated transmission of the combined BF and etalons over the spectral regime of 2700 nm–2850 nm.

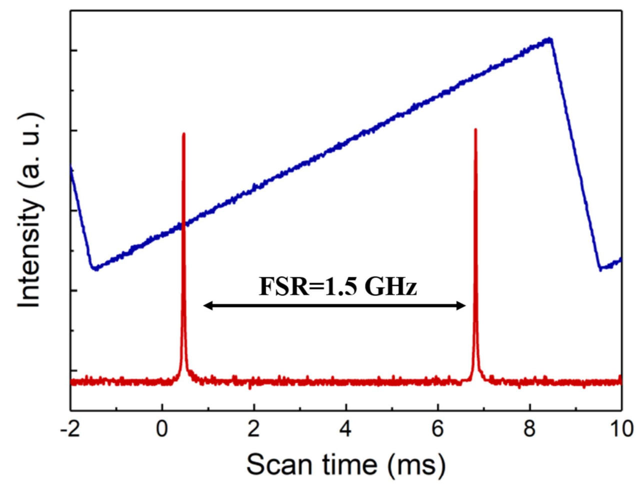

Fig. 4. A typical trace of the FPI scan.

of Fig. 2(a). The corresponding emission peaks were located at ∼2709 nm, ∼2717 nm, ∼2725 nm, and ∼2740 nm and an obvious red-shift behavior was observed with increasing pump power. Over an output power of ∼330 mW, ∼2740 nm was dominated with a linewidth of ∼0.3 nm, which is ∼5 times the longitudinal mode separation of the resonator.

To realize SLM laser operation, two etalons and a quartz BF were inserted into the resonator simultaneously. Mode selecting capability of etalons in the resonator depends on the thickness and refractive index of the etalons and BF. The refractive index of YAG is ∼1.788, which corresponds to Fresnel reflection of ∼8% per facet. Theoretical transmission of the combined two etalons and BF (blue curve) for a given wavelength in comparison with the longitudinal mode separation of the resonator is depicted in Fig. 3(a). It should be noted that, the F-P effects induced by the uncoated ceramic (red curve) should be favorable for SLM laser oscillation. As shown in Fig. 3(a), only one longitudinal mode can locate at the transmission peak and get enough gain to oscillate. The modes deviated from the transmission peak will be suppressed due to the enlarged difference in loss between different modes during oscillation process.

By properly adjusting the tilting angle of the etalons and carefully optimizing the resonator, stable SLM laser operation can be achieved. Lasing threshold occurred at an absorbed pump power of ∼1.7 W, and the SLM laser output as a function of absorbed pump power is shown in Fig. 2(a) (triangles). It was found that stable SLM laser operation could be maintained at 240 mW of output power at an absorbed pump power of 5.1 W, corresponding to a slope efficiency of 6.0% with respect to the absorbed pump power. Output power stability was recorded in 10 minutes, as shown in Fig. 2(b), and the amplitude fluctuation was estimated to be ∼0.78% (RMS). It should be noted that slightly adjustment of resonator may be needed during the experiment to maintain SLM operation due to thermal lensing effect of the ceramic at different pump power levels. As the absorbed pump power increased above 5.1 W, the adjacent longitudinal modes reach lasing threshold and mode competition occurred due to the inherent spatial hole burning. Mode hoping occurs at the wavelength tuning stage when the resonator and/or intracavity components adjusted or the pump power level changed. Stable SLM operation could be maintained once the laser reaches thermal and machinal stabilization. SLM operation with improved output power level should be achievable with modified resonator design of improved mode selectability, such as with VBG and etalon combination.

Single longitudinal mode operation was confirmed using a scanning Fabry–Perot interferometer (FPI; Thorlabs, SA210-18C) of 1.5 GHz free spectral range (FSR). At an output power of 240 mW, the typical trace of the FPI scan is shown in Fig. 4. The linewidth was estimated to be ∼10 MHz. SLM operation was maintained throughout the whole measurement and no additional longitudinal mode observed.

Wavelength tuning was achieved by slightly altering the angle between the optical axis and the ray traveling inside the BF mounted on a precise rotator. Fig. 3(b) shows the simulated transmission of the combined BF and intracavity etalons at a rotating angle of 42° over the spectral regime of 2700 nm–2850 nm. As can be seen, wavelength of 2725.7 nm has the maximum transmission at this angle and similar simulation can be done for other possible emission lines. Experimentally, SLM laser operation with tuning range of 2708.6 nm–2741.2 nm was achieved and due to the relatively sharp emission spectrum of Er:Y_2O_3 ceramic, tuning curves were discrete with range from 2708.6 nm–2710.4 nm, 2715.7 nm–2717.6 nm, 2724.8 nm–2727.4 nm, 2739.5 nm–2741.2 nm. Fig. 5(a) shows the output power at different tuning wavelengths of the SLM laser at an absorbed pump power of 5.1 W. The maximum SLM output power was 240 mW at 2717 nm. It's worth noting that output power level of the SLM varies only slightly with wavelength tuning, and maintained at more than 220 mW throughout the whole tuning range. Further improvement of tunability could be achievable using wavelength selectors with improved selectability in the

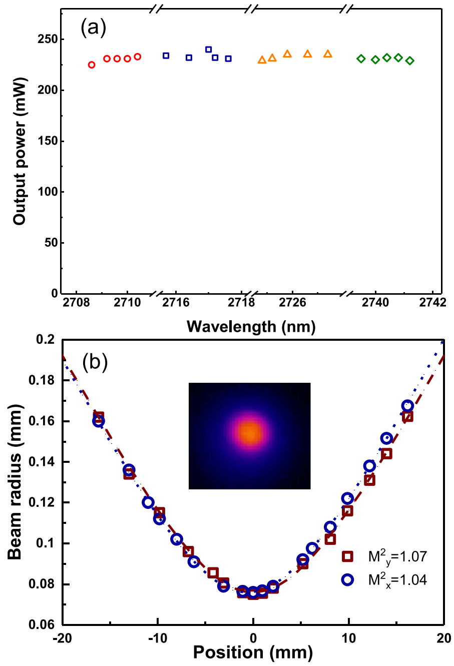

Fig. 5. (a) Output power vs. operating wavelength of single longitudinal mode $Er{:}Y_2O_3$ ceramic laser and (b) measured M^2-factor of the $Er{:}Y_2O_3$ ceramic laser. Inset in (b): transverse beam profile.

resonator, such as VBGs. The polarization extinction ratio (PER) was measured to be ∼20 dB at the maximum output power.

Fig. 5(b) shows the measured transverse profiles and beam radius of the $Er{:}Y_2O_3$ laser at an output power of ∼240 mW using a CCD camera (Xenics, Tigris-640) after passing through a focal lens of 150 mm. The laser beam exhibits a typical Gaussian beam distribution and the beam quality (M^2) was measured to be 1.04 and 1.07 in the horizontal and vertical directions, respectively.

IV. Conclusion

In conclusion, we have demonstrated single longitudinal mode and wavelength tunable operation of an $Er{:}Y_2O_3$ ceramic laser at ∼2.7 μm using intracavity Fabry-Perot etalons and birefringent filter as longitudinal mode and wavelength selector. The $Er{:}Y_2O_3$ ceramic was home-developed and has an Er^{3+} doping level of 3.0 at.%. The laser generated 240 mW of single frequency output power for an absorbed pump power of 5.1 W. The wavelength tuning range was demonstrated from 2708.6 nm–2741.2 nm, with output powers larger than 220 mW over the whole tuning range. The polarization extinction ratio was ∼20 dB at the maximum output power. Such tunable SLM laser source in the ∼3 μm regime are interesting for applications in spectroscopy analysis.

References

[1] F. K. Tittel, D. Richter, and A. Fried, "Mid-Infrared laser applications in spectroscopy," in *Solid-state Mid-Infrared Laser Sources*, I. T. Sorokina and K. L. Vodopyanov eds., New York, NY, USA: Springer, 2003, pp. 458–529.

[2] R. C. Stoneman, J. G. Lynn, and L. Esterowitz, "Direct upper-state pumping of the 2.8 μm Er^{3+}:YLF laser," *IEEE J. Quantum Elect.*, vol. 28, no. 4, pp. 1041–1045, Apr. 2002.

[3] B. J. Dinerman and P. F. Moulton, "3-μm CW laser operations in erbium-doped YSGG, GGG, and YAG," *Opt. Lett.*, vol. 19, no. 15, pp. 1143–1145, 1994.

[4] J. G. Sousa, D. Welford, and J. Foster, "Efficient 1.5 W CW and 9 mJ quasi-CW TEM00 mode operation of a compact diode-laser-pumped 2.94-μm Er:YAG laser," *Proc. SPIE*, 2010, vol. 7578, pp. 346–353.

[5] W. C. Yao, H. Uehara, H. Kawase, H. J. Chen, and R. Yasuhara, "Highly efficient Er: YAP laser with 6.9 W of output power at 2920 nm," *Opt. Exp.*, vol. 28, no. 13, pp. 19000–19007, 2020.

[6] A. Dergachev and P. F. Moulton, "Tunable CW Er:YLF diode-pumped laser," in *Proc. Adv. Solid-State Photon.*, 2003, Art. no. 3.

[7] T. T. Basiev et al., "Continuously tunable CW lasing near 2.75 μm in diode-pumped $Er^{3+}:SrF_2$ and $Er^{3+}:CaF_2$ crystals," *Quantum Electron.*, vol. 36, no. 7, pp. 591–594, 2006.

[8] C. Kränkel, "Rare-earth-doped sesquioxides for diode-pumped high-power lasers in the 1-, 2-, and 3-μm spectral range," *IEEE J. Sel. Topics Quantum Electron.*, vol. 21, no. 1, Jan./Feb. 2015, Art. no. 1602013.

[9] T. Li, K. Beil, C. Kränkel, and G. Huber, "Efficient high-power continuous wave $Er{:}Lu_2O_3$ laser at 2.85 μm," *Opt. Lett.*, vol. 37, no. 13, pp. 2568–2670, 2012.

[10] M. G. Fan et al., "Watt-level passively Q-switched Er: Lu_2O_3 laser at 2.84 μm using MoS_2," *Opt. Lett.*, vol. 41, no. 3, pp. 540–543, 2016.

[11] A. Ikesue and Y. L. Aung, "Ceramic laser materials," *Nature Photon.*, vol. 2, no. 12, pp. 721–727, 2008.

[12] J. Mužík, R. Yasuhara, M. Smrž, V. Kubeček, and T. Mocek, "A high-brightness room temperature 2.7 μm Er: Y_2O_3 ceramic laser," *Laser Phys. Lett.*, vol. 16, no. 3, 2019, Art. no. 035801.

[13] T. Sanamyan, "Diode pumped cascade $Er{:}Y_2O_3$ laser," *Laser Phys. Lett.*, vol. 12, no. 12, 2015, Art. no. 125804.

[14] H. Uehara et al., "Optimization of laser emission at 2.8 μm by Er: Lu_2o_3 ceramics," *Opt. Exp.*, vol. 26, no. 3, pp. 3497–3507, 2018.

[15] W. C. Yao et al., "LD-pumped 2.8 μm $Er{:}Lu_2O_3$ ceramic laser with 6.7 W output power and >30% slope efficiency," *Appl. Phys. Exp.*, vol. 14, no. 1, pp. 1–4, 2021.

[16] Z. P. Qin, G. Q. Xie, J. Zhang, J. G. Ma, P. Yuan, and L. J. Qian, "Continuous-wave and passively Q-switched Er: Y_2O_3 ceramic laser at 2.7 μm," *Int. J. Opt.*, vol. 2018, pp. 1–5, 2018.

[17] L. Wang, H. T. Huang, D. Y. Shen, J. Zhang, H. Chen, and D. Y. Tang, "Diode-pumped high power 2.7 μm $Er{:}Y_2O_3$ ceramic laser at room temperature," *Opt. Mater.*, vol. 71, pp. 70–73, 2017.

[18] Z. D. Fleischman and T. Sanamyan, "Spectroscopic analysis of $Er^{3+}:Y_2O_3$ relevant to 2.7μm mid-IR laser," *Opt. Mater. Exp.*, vol. 6, no. 10, pp. 3109–3118, 2016.

[19] Z. Y. You et al., "Single-longitudinal-mode Er: GGG microchip laser operating at 2.7 μm," *Opt. Lett.*, vol. 40, no. 16, pp. 3846–3849, 2015.

[20] B. Q. Yao, F. Chen, C. H. Zhang, Q. Wang, C. T. Wu, and X. M. Duan, "Room temperature single-frequency output from a diode-pumped Tm, Ho: YAP laser," *Opt. Lett.*, vol. 36, no. 9, pp. 1554–1556, 2011.

[21] L. Wang, C. Q. Gao, M. W. Gao, and Y. Li, "Resonantly pumped monolithic nonplanar Ho: YAG ring laser with high-power single-frequency laser output at 2122 nm," *Opt. Exp.*, vol. 21, no. 8, pp. 9541–9546, 2013.

[22] Y. J. Wang, W. H. Yang, H. J. Zhou, M. R. Huo, and Y. H. Zhen, "Temperature dependence of the fractional thermal load of ND: YVO_4 at 1064 nm lasing and its influence on laser performance," *Opt. Exp.*, vol. 21, no. 15, pp. 18068–18078, 2013.

[23] E. Wu, H. Pan, S. Zhang, and H. Zeng, "High power single-longitudinal-mode operation in a twisted-mode-cavity laser with a C-cut ND: $GdVO_4$ crystal," *Appl. Phys. B*, vol. 80, no. 4, pp. 459–462, 2005.

[24] X. X. Li et al., "High power single frequency $TM{:}Y_2O_3$ ceramic laser at 2015 nm," *IEEE Photon. J.*, vol. 13, no. 3, Jun. 2021, Art. no. 1500207.

[25] Y. S. Zhang et al., "Single-mode oscillations of diode-pumped mid-infrared $Er{:}Y_2O_3$ ceramic microchip lasers at 2.7 μm," *Opt. Exp.*, vol. 27, no. 22, pp. 31783–31789, 2019.

[26] D. L.Yin et al., "Fabrication of $Er{:}Y_2O_3$ transparent ceramics for 2.7 μm mid-infrared solid-state lasers," *J. Eur. Ceram. Soc.*, vol. 40, no. 2, pp. 444–448, 2020.